Synthesis, Reactivity, and the Electronic Structures of Fluoro- and Hydridophosphazene Anions: X-ray Crystal Structure of $[Li(THF)_3][N_3P_3F_2H(BEt_3)(\eta\text{-}C_5H_4)_2Fe]$[1]

Harry R. Allcock,* William D. Coggio, Ian Manners, and Masood Parvez

Department of Chemistry, The Pennsylvania State University, University Park, Pennsylvania 16082

Received November 13, 1990

The reaction of $(NPF_2)_3$ with 2.0 equiv of $Li[BEt_3H]$ in THF at 25 °C yields a triethylborane-stabilized fluorophosphazene anion $[N_3P_3F_5BEt_3]^-$. This species possesses a nucleophilic P(V) center that reacts readily with organic halides such as MeI or $PhCH_2Br$, with CF_3CH_2OH as a proton source, or with organometallic halides such as $CpFe(CO)_2I$ to produce $N_3P_3F_5Me$, $N_3P_3F_5CH_2Ph$, $N_3P_3F_5H$, or $N_3P_3F_5Fe(CO)_2Cp$, respectively. The remaining fluorine atoms in these products were replaced by trifluoroethoxy groups to facilitate characterization. Reaction of $(NPF_2)_3$ with 3 equiv of $Li[BEt_3H]$ in THF or reaction of the fluorophosphazene anion, $[N_3P_3F_5BEt_3]^-$, with 1 equiv of $Li[BEt_3H]$ generated a hydridophosphazene anion $[N_3P_3F_4HBEt_3]^-$. Similarly, reaction of the transannular ferrocenyl species $N_3P_3F_4(\eta\text{-}C_5H_4)_2Fe$ with 3 equiv of $Li[BEt_3H]$ in THF produced the hydridophosphazene anion $[N_3P_3F_2H(BEt_3)(\eta\text{-}C_5H_4)_2Fe]^-$ in high yield. The electronic structures of the hydridophosphazene anions $[N_3P_3F_4HBEt_3]^-$ or $[N_3P_3F_2H(BEt_3)(\eta\text{-}C_5H_4)_2Fe]^-$ appear to differ significantly from that of the fluorophosphazene anion $[N_3P_3F_5BEt_3]^-$. Spectroscopic and reactivity studies suggest that the phosporus atom in the hydrido species exists in the +3 oxidation state, with the negative charge residing mainly on skeletal nitrogen. This situation is supported by the X-ray diffraction study of the hydridophosphazene anion $[N_3P_3F_2H(BEt_3)(\eta\text{-}C_5H_4)_2Fe]^-[Li(THF)_3]^+$, in which the lithium cation is coordinated to a skeletal nitrogen atom and is also surrounded by three THF molecules. Crystals of this compound are monoclinic, with a $P2_1/c$ space group and with a = 11.363 (3) Å, b = 27.701 (9) Å, c = 11.667 (5) Å, β = 115.42 (4)°, V = 3316.8 Å^3, and Z = 4.

One of the most useful synthetic reactions available for halogenophosphazenes is the replacement of side group halogen atoms by nucleophiles such as aryloxides, alkoxides, or amines.[2,3] This method has allowed the preparation of a broad range of cyclic, linear, and macromolecular derivatives. By contrast, the reactions of halogenophosphazenes with organometallic, or transition-metal nucleophiles are often complex.[4-6] In particular, these reactions are seldom efficient at the macromolecular level because of chain cleavage, incomplete substitution, or side reactions that result in cross-linking. An alternative approach to the attachement of organic, organometallic, or transition-metal side groups to a phosphazene skeleton involves the generation of phosphazene anions which contain nucleophilic skeletal phosphorus atoms that react readily with electrophiles.[7-13] These species have considerable synthetic utility because they avoid many of the side reactions associated with the use of organometallic reagents. Indeed, since their discovery in 1979, phosphazene anions have been exploited to produce a variety of novel organo and organometallic cyclotriphosphazenes that are either difficult or impossible to synthesize by other routes.

Several different types of phosphazene anions are known, each possessing a nucleophilic phosphorus atom but with different degrees of reactivity and stability. The first phosphazene anion synthesized, **1**, was obtained by

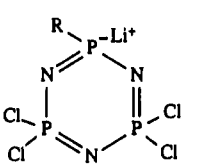

1

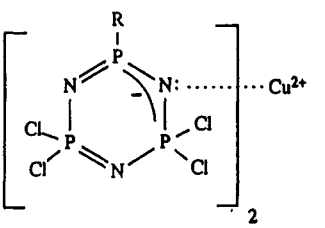

2

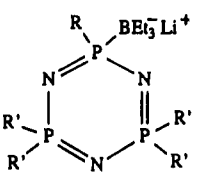

3, R' = Cl, OCH_2CF_3

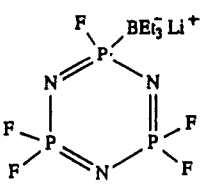

6

the low-temperature deprotonation of a hydridophosphazene with ^{n}BuLi.[12] It was later discovered that anionic phosphazenes could be generated by the reaction

(1) Some of the results described in this paper have been reported previously in a preliminary communication: Manners, I.; Coggio, W. D.; Mang, M. N.; Parvez, M.; Allcock, H. R. *J. Am. Chem. Soc.* **1989**, *111*, 3481.

(2) Allcock, H. R. *Chem. Eng. News* **1985**, *63* (March 18), 22.

(3) Allcock, H. R. *Phosphorus-Nitrogen Compounds*; Academic Press: New York, 1972.

(4) Ritchie, R. J.; Harris, P. J.; Allcock, H. R. *Inorg. Chem.* **1980**, *19*, 2483.

(5) Evans, T. L.; Patterson, D. B.; Suszko, P. R.; Allcock, H. R. *Macromolecules* **1981**, *14*, 218.

(6) Allcock, H. R.; Desorcie, J. L.; Riding, G. H. *Polyhedron* **1987**, *6*, 119.

(7) Allcock, H. R.; Connolly, M. S.; Whittle, R. R. *Organometallics* **1983**, *2*, 1514.

(8) Allcock, H. R.; Manners, I.; Mang, M. N.; Parvez, M. *Inorg. Chem.* **1990**, *29*, 522.

(9) Nissan, R. A.; Connolly, M. S.; Mirabelli, M. G. L.; Whittle, R. R.; Allcock, H. R. *J. Chem. Soc., Chem. Commun.* **1983**, 822.

(10) Allcock, H. R.; Mang, M. N.; Riding, G. H.; Whittle, R. R. *Organometallics* **1986**, *5*, 2244.

(11) Allcock, H. R.; Mang, M. N.; McDonnell, G. S.; Parvez, M. *Macromolecules* **1987**, *20*, 2060.

(12) Allcock, H. R.; Harris, P. J. *J. Am. Chem. Soc.* **1979**, 101, 6221.

(13) Allcock, H. R.; Harris, P. J.; Connolly, M. S. *Inorg. Chem.* **1981**, *20*, 11.

0276-7333/91/2310-3090$02.50/0

Scheme I

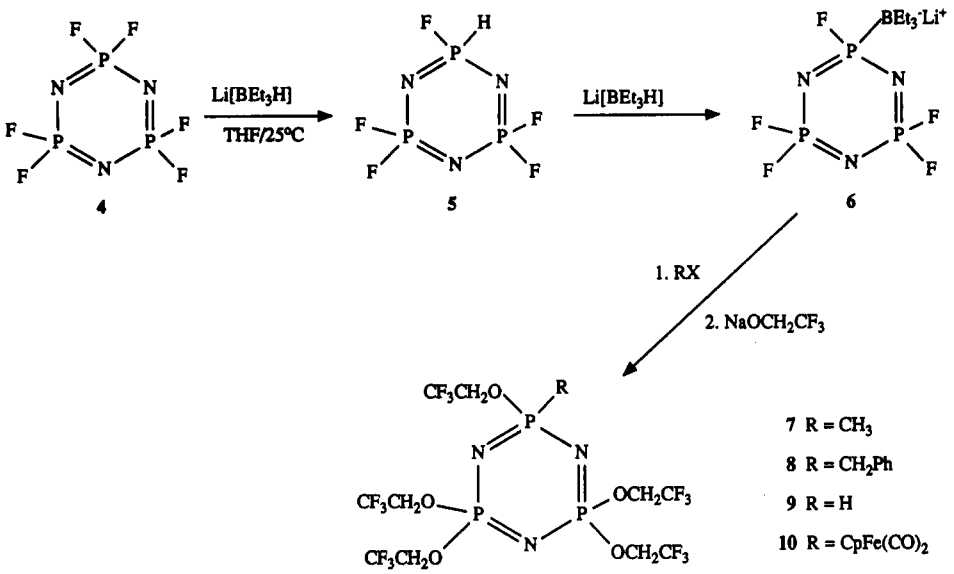

between alkyl Grignard reagents and chlorophosphazenes in the presence of an alkylcopper phosphine reagent.[13] The structure of these anionic species was not clearly defined, but those generated by the organocopper route were believed to exist as dimers stabilized by the (tri-*n*-butylphosphine)cuprate ligand **2**.[13,14] However, species **1** is not stable above −50 °C, and it is, therefore, of limited synthetic utility. Furthermore, although species **2** is stable at room temperature, it possesses a relatively low reactivity. Thus, these intermediates react only with sterically unhindered iodoalkanes.

An important synthetic advance resulted from the discovery that the naked anion **1** could be stabilized by coordination of BEt_3 to produce phosphazene anions of the type **3**. It was found that these anionic species were stable at temperatures up to 66 °C.[10,11] Thus, reactions with a wider range of electrophiles became possible as a result of this increased thermal stability. In recent years, this chemistry has been used for the synthesis of new cyclophosphazene polymerization monomers and novel organometallic polyphosphazenes.[10,11,15]

Despite their considerable potential, the use of phosphazene anions has been limited. Drawbacks such as the experimental conditions needed for their generation, low loadings of active sites (i.e. only one anionic site per phosphazene ring), and the difficulty experienced in obtaining high polymeric phosphazene anions (electronegative trifluoroethoxy cosubstituents are required in order for these anions to form[11]) have hampered their use. In addition, the electronic structure of phosphazene anions has remained unclear. Thus, in certain aspects of their chemistry, they appear to possess a phosphorus(III) center.[14]

In this paper we describe an investigation into the synthesis, structure, and reactivity of phosphazene anions derived from *fluoro*phosphazenes. It appeared possible that the electronegative fluoro side units would facilitate phosphazene anion formation, and this might allow more nucleophilic sites to be generated per phosphazene ring.

(14) Other workers have suggested that the copper ligand in species **2** occupies a position on a skeletal phosphorus atom and not on skeletal nitrogen. Although some data exist to support this argument, the correct structure of **2** is still a matter of debate. See: Buwalda, P. L.; Steenberger, A.; Oosting, G. E.; van der Grample, J. C. *Inorg. Chem.* **1990**, *29*, 2658.

(15) Allcock, H. R.; Ritchie, R. J.; Harris, P. J. *Macromolecules* **1980**, *13*, 1325.

Results and Discussion

Synthesis of the Fluorophosphazene Anion $[N_3P_3F_5BEt_3]^-$ (6). The addition of 2.0 equiv of a solution of $Li[BEt_3H]$ in THF to $(NPF_2)_3$ (**4**) in the same solvent at 25 °C led to the smooth evolution of hydrogen. After 1 h, analysis of the reaction mixture by ^{31}P NMR spectroscopy indicated that a new product, **6**, had formed (see Scheme I and Figure 1a–c). A ^1H-decoupled ^{31}P NMR spectrum of **6** (Figure 1c) contained a broad, low-field doublet resonance (δ = 100 ppm, J_{PF} = 1020 Hz) assigned to a skeletal phosphorus atom that bears both fluorine and triethylborane substituents, together with a triplet resonance (δ = 8.0 ppm) characteristic of PF_2 groups (J_{PF} = 1020 Hz). The ^1H-coupled ^{31}P NMR spectrum of this species was essentially identical with the one shown in Figure 1c, which suggested that no hydrido substituents were bonded to the phosphorus atoms. Side reactions, such as dimerization and formation of the hydridophosphazene anion **11** (discussed later), were avoided by use of low concentration of reagents at 25 °C. Once formed, solutions of the fluorophosphazene anion **6** were stable for up to 1 week under an inert atmosphere but decomposed slowly in the presence of air or moisture.

The mechanism for the formation of **6** probably involves an initial replacement of fluorine by hydrogen to give species **5**, followed by rapid deprotonation and coordination of BEt_3 to phosphorus (Scheme I). This mechanism is consistent with both the reaction stoichiometry and the previously observed deprotonation reaction of hydridophosphazenes with $Li[BEt_3H]$ to give phosphazene anions.[12] However, no evidence for intermediate **5** was detected. Addition of 1.0 equiv of $Li[BEt_3H]$ to $(NPF_2)_3$ yielded only a 1:1 mixture of **6** and unreacted starting material **4** (see Figure 1b). This suggests that the initial step, which involves fluorine atom replacement by hydrogen to yield **5**, is also the rate-determining step.

Reaction of the Fluorophosphazene Anion 6 with Electrophiles. The reactions between **6** and electrophiles are depicted in Scheme I. The fluorophosphazene anion **6** appeared to behave in a manner similar to that of classical organic nucleophiles. Thus, **6** reacted readily with species such as benzyl bromide, methyl iodide, trifluoroethanol or cyclopentadienyldicarbonyliron iodide, $CpFe(CO)_2I$, during a 6–12-h period at room temperature to produce the corresponding monosubstituted pentafluorocyclotriphosphazenes in high yields. The products were

Table I. Characterization Data for $N_3P_3(OCH_2CF_3)_5R$ (7–10)

	^{31}P NMR[a]		^1H NMR		^{13}C NMR	
R	signal	δ, ppm	signal	δ, ppm	signal	δ, ppm
CH_3 (7)	$P(OCH_2CF_3)R$	40.0 (t)	OCH_2CF_3[b]	4.3 (m)	OCH_2CF_3	62.7 (q, $^2J_{CF}$ = 38.0 Hz)
	$P(OCH_2CF_3)_2$	15.7 (d)	CH_3	1.6 (d)	OCH_2CF_3	129.9 (q, J_{CF} = 188.4 Hz)
		($^2J_{PP}$ = 48.8 Hz)		($^2J_{PH}$ = 16.9 Hz)	CH_3	16.9 (d, J_{CP} = 146.3 Hz)
CH_2Ph (8)	$P(OCH_2CF_3)R$	38.3 (t)	OCH_2CF_3 (trans)	4.3 (m)	OCH_2CF_3	63.0 (q, $^2J_{CF}$ = 37.4 Hz)
	$P(OCH_2CF_3)_2$	15.7 (d)	OCH_2CF_3 (cis)	3.7 (m)	OCH_2CF_3	124.0 (q, J_{CF} = 280.0 Hz)
		($^2J_{PP}$ = 43.9 Hz)	CH_2	3.2 (d, t)	CH_2	37.1 (d, t, J_{CP} = 139.8 Hz)
				($^2J_{PH}$ = 22.2 Hz)		
			Ph	7.3 (s)	Ph	128–131 (m)
H (9)[c]	$P(OCH_2CF_3)R$	−0.3 (t)	OCH_2CF_3	4.3 (m)	OCH_2CF_3	63.0 (q, $^2J_{CF}$ = 38.0 Hz)
	$P(OCH_2CF_3)_2$	17.2 (d)	H	7.0 (d, t)	OCH_2CF_3	125.6 (q, J_{CF} = 190.0 Hz)
		($^2J_{PP}$ = 46.7 Hz, J_{PH} = 595 Hz)				
$CpFe(CO)_2$ (10)[d]	$P(OCH_2CF_3)R$	117.7 (t)	OCH_2CF_3 (trans)	4.3 (m)	OCH_2CF_3	63.0 (q, $^2J_{CF}$ = 40.0 Hz)
	$P(OCH_2CF_3)_2$	9.9 (d)	OCH_2CF_3 (cis)	3.8 (m)	OCH_2CF_3	124.0 (q, J_{CF} = 125.0 Hz)
		($^2J_{PP}$ = 43.9 Hz)	C_5H_5	5.0 (s)	C_5H_5	86.0 (s)

[a] NMR spectra recorded in $CDCl_3$ solutions. [b] cis/trans signals for OCH_2CF_3 groups were not resolved; the reported value represents the average chemical shift of the signal. [c] IR spectra showed a strong P–H stretch at 2390 cm^{-1}. [d] IR spectra recorded in CH_2Cl_2 solutions: strong bands at 2040 and 1990 cm^{-1} for CO groups were detected.

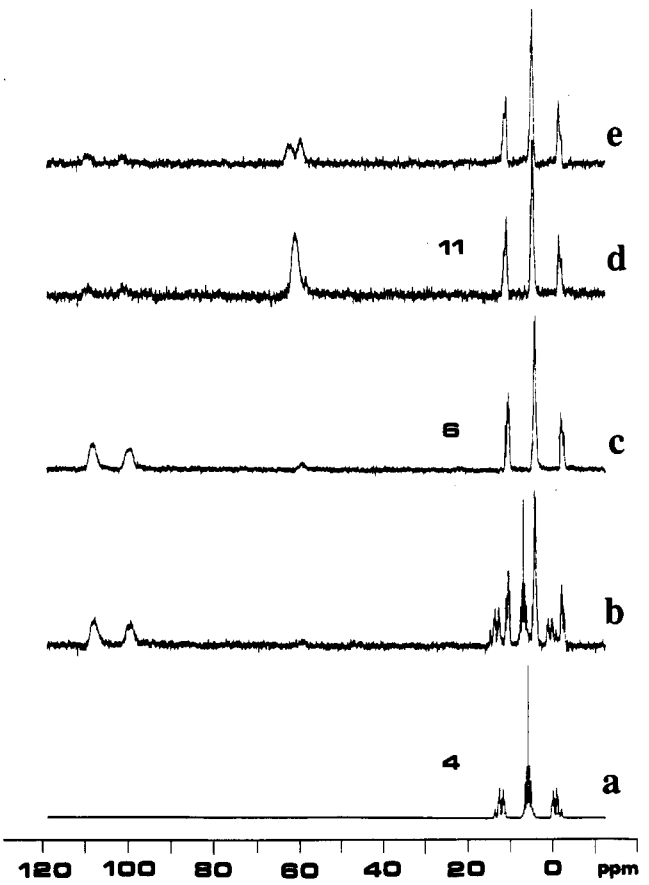

Figure 1. 145.8-MHz ^{31}P NMR spectra for the reaction between $(NPF_2)_3$ (4) and $Li[BEt_3H]$. (a) Spectrum of 4 before addition of $Li[BEt_3H]$. (b) Spectrum of the reaction mixture taken after the addition of 1.0 equiv of $Li[BEt_3H]$ to a THF solution of 4. (c) Spectrum of the reaction mixture taken after the addition of 2.0 equiv of $Li[BEt_3H]$ to 4. (d) Spectrum of 11, formed by the addition of 3.0 equiv of $Li[BEt_3H]$ to 4. The peak at 62 ppm represents the hydridophosphazene anion. (e) Proton-coupled ^{31}P NMR spectrum of 11 showing the P–H coupling (J_{PH} = 320 Hz).

then treated in situ with sodium trifluoroethoxide to produce hydrolytically stable trifluoroethoxy derivatives and to facilitate characterization. The resultant products $N_3P_3(OCH_2CF_3)_5R$ where R = CH_3 (7), CH_2Ph (8), H (9), and $CpFe(CO)_2$ (10) were characterized by ^{31}P, ^1H, and ^{13}C NMR spectroscopy, mass spectrometry, and elemental analysis. These data are listed in Table I. The compounds $N_3P_3(OCH_2CF_3)_5CH_3$ (7) and $N_3P_3(OCH_2CF_3)_5(CpFe(CO)_2)$ (10) have also been prepared by other methods reported previously.[10,12]

Anion 6 reacted faster with electrophiles as the temperature was raised to 66 °C. However, the increased rate of substitution was accompanied by lower yields of the monosubstituted product. The byproducts that formed at the higher temperatures were found to include a complex mixture of ring-linked species. These species had molecular weights as high as 1750, which suggested that as many as three phosphazene rings were linked together. This indicated that, at elevated temperatures, phosphazene anions can participate in fluorine displacement reactions with other cyclic trimer molecules.

Synthesis of Hydridophosphazene Anions $[N_3P_3F_4H(BEt_3)]^-$ (11) and $[N_3P_3F_2H(BEt_3)(\eta\text{-}C_5H_4)_2Fe]^-$ (15). In an attempt to generate two anionic sites on a phosphazene ring, compound 6 was allowed to react further with $Li[BEt_3H]$. Although it was found that 6 did indeed react with additional $Li[BEt_3H]$, the resultant product was *not* the desired fluorophosphazene *di*anion (see Scheme II). The product was identified by ^1H-decoupled and -coupled ^{31}P NMR spectroscopy as the *hydrido*phosphazene anion 11 (see Scheme II). In addition, it was found that species 11 could also be generated directly via the reaction between 4 and 3.0 equiv of $Li[BEt_3H]$ in THF at 25 °C.

The ^1H-decoupled ^{31}P NMR spectrum of 11 (see Figure 1d,e) showed a triplet resonance (δ = 8.0 ppm) characteristic of PF_2 groups and a broad singlet resonance at 62 ppm. The latter resonance split into a doublet in the ^1H-coupled ^{31}P NMR spectrum (J_{PH} = 320 Hz) and was assigned to the skeletal phosphorus atom bearing both hydrogen and a triethylborane substituent.

The formation of 11 from 6 appears to involve a straightforward replacement of the fluorine atom geminal to the triethylborane substituent by hydrogen. This reaction also provided evidence for the first step in the postulated mechanism for the formation of 6 (see Scheme I). Nucleophilic attack by H^- appears to occur specifically at the fluorine atom geminal to the BEt_3 substituent. No evidence for attack on another PF_2 unit in 6 was detected by ^{31}P NMR spectroscopy, despite the high statistical probability that such a reaction should occur. This observation supports further the postulate that attack by H^- on a PF_2 unit is the rate-determining step.

Similarly, reaction of 3.0 equiv of $Li[BEt_3H]$ with 1,1,3,5-tetrafluoro-3,5-(transannular ferrocenyl)cyclotriphosphazene (12) in THF gave the hydridophosphazene

Scheme II

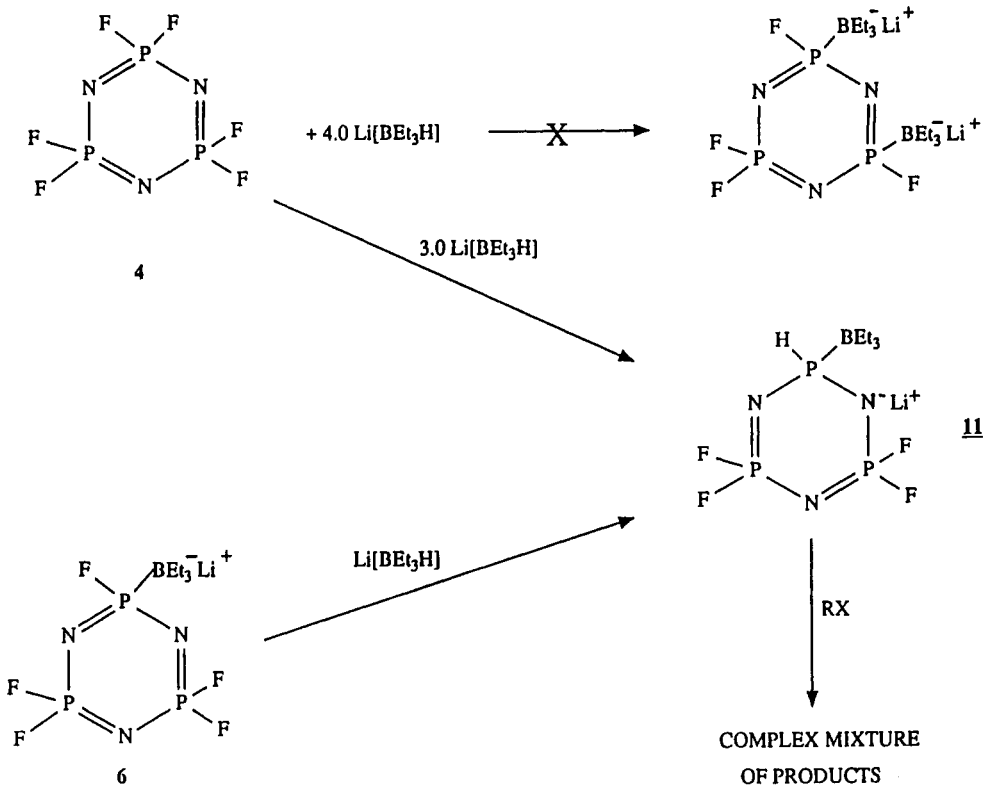

Scheme III

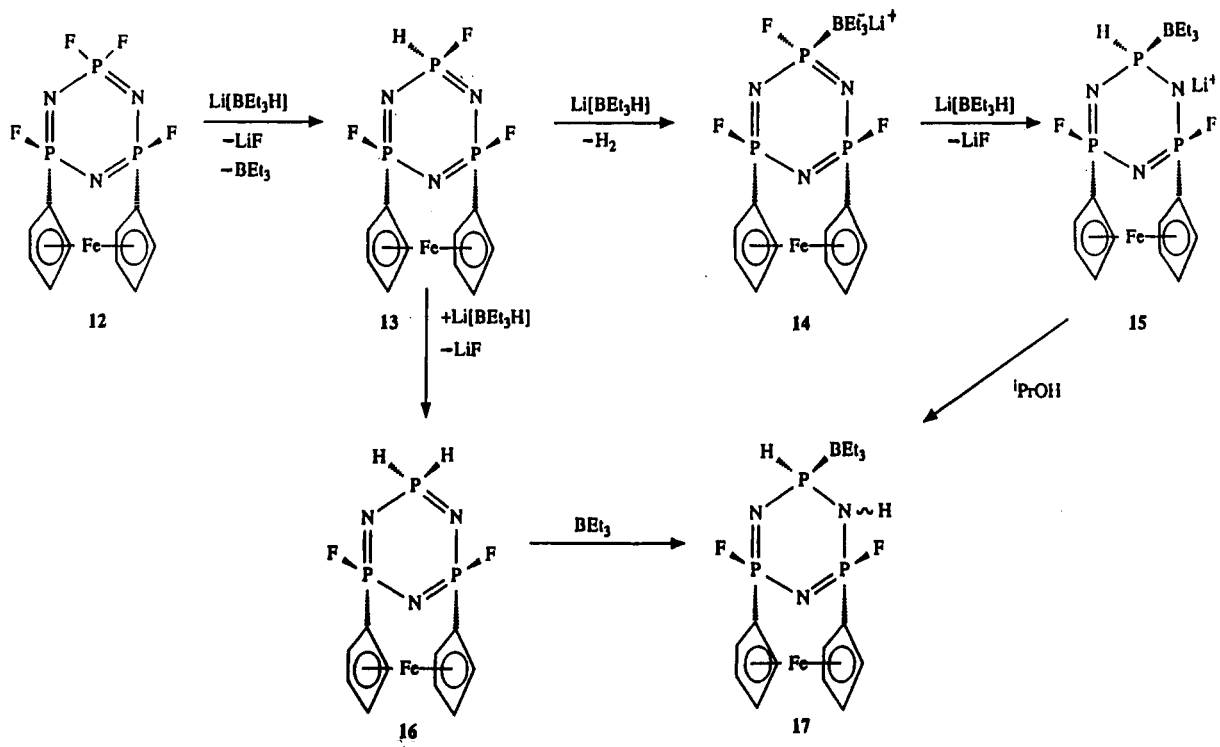

anion **15** in ca. 75% yield, based on ^{31}P NMR spectroscopy (see Scheme III). This reaction was monitored readily by ^{31}P NMR spectroscopy, and typical ^{31}P NMR spectra for this process are shown in Figure 2a–e. In addition to the major product, **15**, at least two other minor products were formed. The formation of these species will be discussed later.

The formation of **15** can be explained by a mechanism similar to the one proposed for the formation of the hydridophosphazene anion **11** from $(NPF_2)_3$ (see Scheme III).[16] The ^1H-decoupled ^{31}P NMR spectrum of **15** showed a doublet of doublets at 37.4 ppm that were assigned to skeletal phosphorus atoms which bear both a fluorine atom and a cyclopentadienyl group. In addition, a broad, low-

(16) Although the mechanism outlined in Scheme III suggests that **15** forms via a fluoro anion intermediate (**14**), no such species was detected by ^{31}P NMR spectroscopy. In reactions that involved **12** and 2.0 equiv of Li[BEt_3H] only a mixture of starting material and **15**, **17**, and **18** was detected.

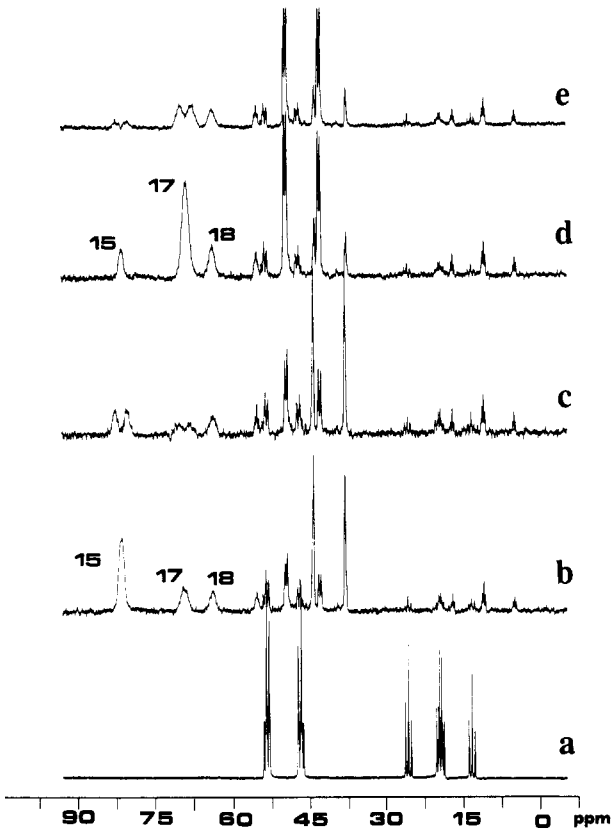

Figure 2. 145.8-MHz ^{31}P NMR spectra for the reaction between **12** and $Li[BEt_3H]$ in THF at 25 °C. (a) Spectrum of **12** before the addition of $Li[BEt_3H]$. (b) Spectrum of the reaction mixture after the addition of 3.0 equiv of $Li[BEt_3H]$ to **12**. Because of coupling to boron, broad signals appear at 78.0 ppm for **15**, 68.0 ppm for **17** and 58.0 ppm for **18**. (c) Proton-coupled ^{31}P NMR spectrum of the reaction mixture, showing the P–H coupling (J_{PH} = 320 Hz). (d) Spectrum of the reaction mixture after the addition of $^{i}PrOH$. Note the increase in the intensity of the signal for the resonance associated with **17**. (e) Proton-coupled spectrum after the addition of $^{i}PrOH$ to the reaction mixture.

field resonance at 78.0 ppm was present (see Figure 2b). The latter resonance split into a doublet in the ^1H-coupled ^{31}P NMR spectrum (J_{PH} = 344 Hz) and was assigned to the skeletal phosphorus atom that bore hydrogen and triethylborane substituents (see Figure 2c).

Reactivity of Hydridophosphazene Anions. In contrast to the fluorophosphazene anion **6**, hydridophosphazene anions **11** and **15** reacted with organic electrophiles such as MeI and $PhCH_2Br$ to give a complex mixture of what were presumed to be phosphazene ring-opened products, as deduced by ^{31}P NMR spectroscopy. Attempts to react **11** or **15** with electrophiles even at temperatures as low as −80 °C gave similar results. These observations suggested that species **11** or **15** did not possess a nucleophilic phosphorus center. Further studies on the electronic structure of these spcies (discussed later) suggested that the phosphorus atom in **11** or **15** had been reduced to the +3 oxidation state.

However, unlike **11**, the hydrido anion derived from the transannular ferrocenyl species (**15**) reacted cleanly with 2-propanol as a proton source, to give compound **17** as a single new product. The ^1H-decoupled and -coupled ^{31}P NMR spectra of **17** were essentially identical with those of **15**, except that the resonances appeared at higher field (see Figures 2d,e). This is consistent with protonation at a skeletal nitrogen atom to afford a neutral product.

Competing Side Reactions. As is evident from Figure 2b, at least two other minor products, in addition to **15**, were formed during the reaction between $Li[BEt_3H]$ and **12**. These products, **17** and **18** (see Scheme IV), were generated in approximately 10% and 15% yield, respectively. Compound **18** formed as a result of a competing reaction between $Li[BEt_3H]$ and a phosphorus atom bonded to the cyclopentadienyl group. The ^{31}P NMR spectrum of **18** consisted of a triplet resonance characteristic of a PF_2 group (δ = 5.0 ppm), a doublet resonance characteristic of a phosphorus atom bonded to both a fluorine atom and a cyclopentadienyl group (δ = 42 ppm), and a broad singlet at 58 ppm assigned to a phosphorus atom bearing a triethylborane and a cyclopentadienyl group (see Figure 2b).

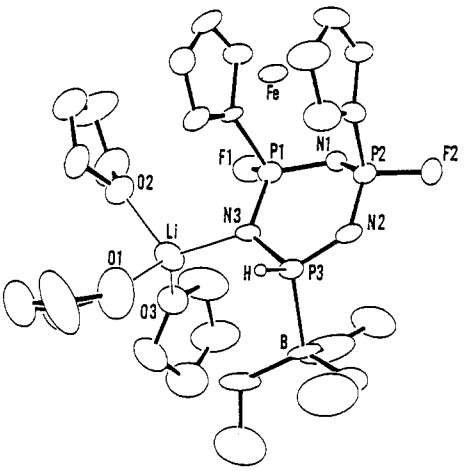

Figure 3. ORTEP structure of **15**, showing the trans arrangement of the BEt_3 unit relative to the transannular ferrocenyl unit.

Compound **17** was identified as a species formally derived from **15** by protonation (see Scheme III). Although **17** can be formed by the addition of $^{i}PrOH$ to a solution of **15** (see Figure 2d and Scheme III), this product, **17**, was detected in the reaction mixture before any proton source was added. This suggests that **17** forms as a result of a competing reaction during the synthesis of **15**. To account for this process, we postulate that **17** may be formed by a mechanism in which intermediate **13** undergoes further fluorine substitution to yield the *gem*-dihydrido species **16**, which subsequently tautomerizes to **17**.

Although it is possible that the formation of **17** may arise by protonation of **15** by traces of water in the reaction mixture, this explanation seems unlikely. It was found that the relative proportion of **15** to **17** was constant and reproducible, as determined by ^{31}P NMR spectroscopy. This suggests that product **17** probably does *not* form as a result of a random, trace amount of water in the reaction mixture, but rather as a result of a competing side reaction with a fixed kinetic rate relative to the formation of **15**. Thus, the mechanism for the formation of **17** via the proposed intermediates **13** and **16** seems reasonable.

The consequence of the addition of 3.0 equiv of $Li[BEt_3H]$ to a THF solution of **12** is shown in Scheme IV. The formation of **17** further supports the postulate that the addition of H^- to a phosphazene can reduce the phosphorus atom(s) to the +3 oxidation state. Further evidence for reduction of the phosphazene ring is discussed later.

X-ray Structure of $[N_3P_3F_2H(BEt_3)(\eta\text{-}C_5H_4)_2Fe]^-$ (15). Before this work, no X-ray structural data on a phosphazene anion existed.[1] A single crystal of **15** suitable for an X-ray diffraction study was grown by cooling a THF/diethyl ether solution to −20 °C in the dark for 14 days. The molecular structure of the lithium salt of **15** is shown in Figure 3. The bond lengths, angles, and posi-

Scheme IV

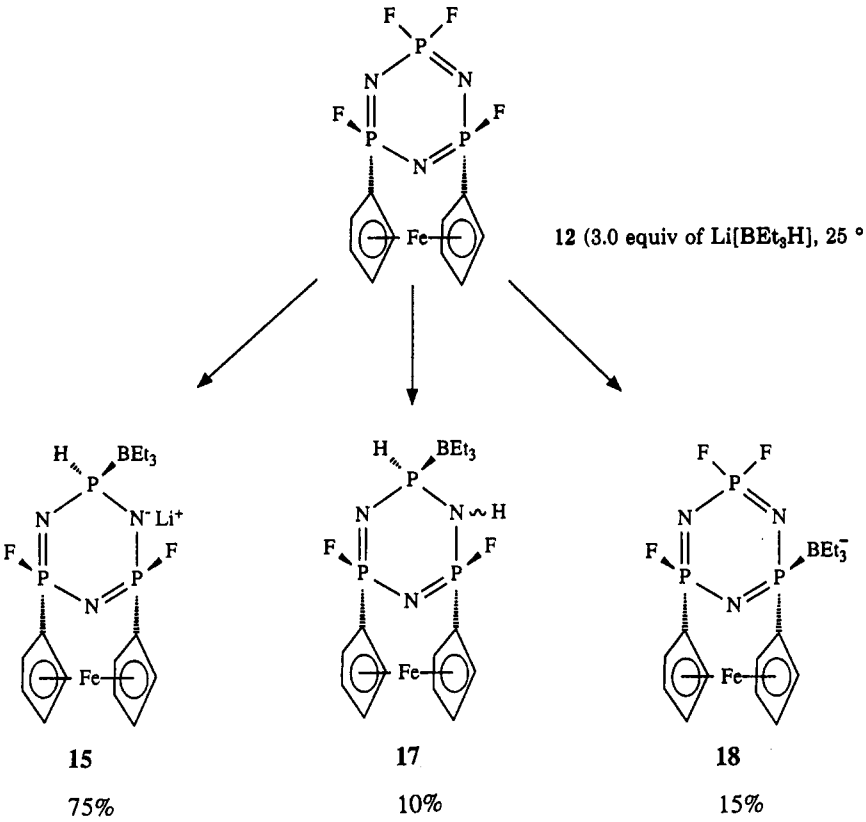

tional parameters are listed in Tables II–IV, respectively. The bond lengths and angles of **15** were also compared to **12** and $(NPF_2)_3$ (**4**) and are listed in Table V. [17c,18]

Two skeletal phosphorus atoms are bonded to both a fluorine atom and a cyclopentadienyl ring of the transannular ferrocenyl group. The remaining skeletal phosphorus atom bears both hydrido and triethylborane substituents. In addition, a skeletal nitrogen atom is coordinated to lithium, which is also bound to three THF molecules. The transannular ferrocenyl and triethylborane groups are located on opposite sides of the phosphazene ring, presumably for steric reasons.

Dramatic differences are found in the bond lengths and angles in the environment of P3 compared to the situation in **12** (see Table IV).[17c,18] Thus, the lengths of the P3–N3 and P3–N2 bonds are 1.74 (6) and 1.626 (5) Å, respectively, which are appreciably longer than the corresponding value of 1.559 (2) Å in **12**. The considerable lengthening of the P3–N3 bond provides excellent structural evidence for the postulate that coordination to skeletal nitrogen atoms by Lewis acids or metals weakens a phosphazene skeletal bond and facilitates cleavage of the phosphorus–nitrogen ring.[19]

The bond lengthening is accompanied by a considerable narrowing of the N2–P3–N3 angle to 112.7 (3)° compared with the value of 120.5 (1)° in **12**. In contrast, the P2–N2–P3 angle is 6° wider with respect to the corresponding angle in **12** (112.8° compared to 118.4 (2)°). Remarkably, the P3–N3–P1 angle (118.7 (3)°) is similar to that in **12** (118.1 (1)°) despite the coordination of lithium to N3. The P3–B bond length is 1.984 (9) Å and is consistent with a single bond.[20]

The geometry of the phosphazene ring in the vicinity of P1, N1, and P2 is similar to that found in **12**. Thus, the phosphazene ring shows considerable deviation from pla-

Table II. Table of Bond Distances (Å) for 19[a]

Fe–C1	2.026 (5)	O3–C28	1.41 (2)
Fe–C2	2.049 (7)	O3–Li	1.97 (1)
Fe–C3	2.063 (8)	N3–Li	2.06 (1)
Fe–C4	2.046 (9)	C1–C2	1.44 (1)
Fe–C5	1.999 (7)	C1–C5	1.44 (2)
Fe–C6	2.036 (8)	C2–C3	1.44 (1)
Fe–C7	2.034 (8)	C3–C4	1.42 (1)
Fe–C8	2.057 (7)	C4–C5	1.41 (1)
Fe–C9	2.025 (7)	C6–C7	1.42 (2)
Fe–C10	2.038 (8)	C6–C10	1.44 (1)
P1–F1	1.558 (4)	C7–C8	1.44 (1)
P1–N1	1.572 (5)	C8–C9	1.42 (1)
P1–N3	1.592 (6)	C9–C10	1.42 (1)
P1–C1	1.766 (9)	C11–C12	1.43 (1)
P2–F2	1.564 (5)	C11–B	1.59 (1)
P2–N1	1.588 (6)	C13–C14	1.49 (2)
P2–N2	1.568 (6)	C13–B	1.61 (1)
P2–C6	1.801 (9)	C15–C16	1.35 (1)
P3–N2	1.626 (5)	C15–B	1.59 (1)
P3–N3	1.674 (6)	C17–C18	1.49 (2)
P3–B	1.984 (9)	C18–C19	1.48 (1)
O1–C17	1.404 (9)	C19–C20	1.38 (2)
O1–C20	1.45 (2)	C21–C22	1.50 (1)
O1–Li	1.97 (1)	C22–C23	1.46 (1)
O2–C21	1.44 (2)	C23–C24	1.49 (2)
O2–C24	1.44 (1)	C25–C26	1.50 (2)
O2–Li	2.01 (2)	C26–C27	1.41 (1)
O3–C25	1.44 (1)	C27–C28	1.50 (2)

[a] Numbers in parentheses are estimated standard deviations in the least significant digits.

(17) (a) Suszko, P. R.; Whittle, R. R.; Allcock, H. R. *J. Chem. Soc., Chem. Commun.* **1982**, 960. (b) Allcock, H. R.; Lavin, K. D.; Riding, G. H.; Suszko, P. R.; Whittle, R. R. *J. Am. Chem. Soc.* **1984**, *106*, 2337. (c) Allcock, H. R.; Lavin, K. D.; Riding, G. H.; Suszko, P. R.; Parvez, M. *Organometallics* **1986**, *5*, 1626.

(18) Dougill, M. W. *J. Chem. Soc. (London)* **1963**, 3211.

(19) Sennett, M. S.; Hagnauer, G. L.; Singler, R. E.; Davies, G. *Macromolecules* **1986**, *19*, 959. For a comprehensive review on phosphazene polymerization see: Hagnauer, G. L. *J. Macromol. Sci. Chem.* **1981**, *A16* (1), 385.

(20) Power, P. P. *Angew. Chem., Int. Ed. Engl.* **1990**, *29*, 449.

Table III. Table of Bond Angles (deg) for 15[a]

C1-Fe-C2	41.3 (3)	P1-N1-P2	110.4 (3)
C1-Fe-C3	69.5 (3)	P2-N2-P3	122.8 (4)
C1-Fe-C4	69.6 (3)	P1-N3-P3	118.7 (3)
C1-Fe-C5	41.8 (3)	P1-N3-Li	113.3 (5)
C1-Fe-C6	107.2 (3)	P3-N3-Li	128.1 (5)
C1-Fe-C7	124.0 (4)	Fe-C1-P1	116.7 (4)
C1-Fe-C8	161.5 (4)	Fe-C1-C2	70.2 (3)
C1-Fe-C9	156.2 (3)	Fe-C1-C5	68.2 (3)
C1-Fe-C10	120.4 (3)	P1-C1-C2	123.7 (6)
C2-Fe-C3	40.9 (3)	P1-C1-C5	128.7 (5)
C2-Fe-C4	68.7 (4)	C2-C1-C5	106.3 (7)
C2-Fe-C5	69.2 (3)	Fe-C2-C1	68.5 (3)
C2-Fe-C6	123.3 (3)	Fe-C2-C3	70.1 (4)
C2-Fe-C7	108.8 (3)	C1-C2-C3	108.3 (6)
C2-Fe-C8	124.7 (4)	Fe-C3-C2	69.1 (5)
C2-Fe-C9	160.4 (3)	Fe-C3-C4	69.1 (5)
C2-Fe-C10	158.2 (3)	C2-C3-C4	107.7 (7)
C3-Fe-C4	40.5 (3)	Fe-C4-C3	70.4 (5)
C3-Fe-C5	68.7 (4)	Fe-C4-C5	67.8 (5)
C3-Fe-C6	159.3 (4)	C3-C4-C5	108.2 (7)
C3-Fe-C7	123.1 93)	Fe-C5-C1	70.1 (4)
C3-Fe-C8	107.6 (3)	Fe-C5-C4	71.4 (4)
C3-Fe-C9	122.9 (4)	C1-C5-C4	109.5 (7)
C3-Fe-C10	158.2 (3)	Fe-C6-P2	114.3 (3)
C4-Fe-C5	40.8 (3)	Fe-C6-C7	69.6 (5)
C4-Fe-C6	159.2 (3)	Fe-C6-C10	69.4 (5)
C4-Fe-C7	157.9 (3)	P2-C6-C7	123.5 (6)
C4-Fe-C8	120.8 (3)	P2-C6-C10	125.4 (5)
C4-Fe-C9	105.8 (3)	C7-C6-C10	109.1 (7)
C4-Fe-C10	121.3 (3)	Fe-C7-C6	69.7 (4)
C5-Fe-C6	123.2 (3)	Fe-C7-C8	70.3 (5)
C5-Fe-C7	160.8 (4)	C6-C70C8	107.8 (7)
C5-Fe-C8	155.7 (3)	Fe-C8-C7	68.5 (4)
C5-Fe-C9	119.7 (3)	Fe-C8-C9	68.4 (4)
C5-Fe-C10	104.8 (4)	C7-C8-C9	106.6 (7)
C6-Fe-C7	40.7 (3)	Fe-C9-C8	70.9 (4)
C6-Fe-C8	68.7 (3)	Fe-C9-C10	70.2 (4)
C6-Fe-C9	68.4 (3)	C8-C9-C10	110.3 (8)
C6-Fe-C10	41.3 (3)	Fe-C10-C6	69.2 (4)
C7-Fe-C8	41.3 (3)	Fe-C10-C9	69.1 (4)
C7-Fe-C9	68.9 (3)	C6-C10-C9	106.2 (7)
C7-Fe-C10	69.6 (3)	C12-C11-B	118.8 (9)
C8-Fe-C9	40.7 (3)	C14-C13-B	116 (1)
C8-Fe-C10	69.3 (3)	C16-C15-B	128.0 (7)
C9-Fe-C10	40.8 (3)	O1-C17-C18	105.5 (6)
F1-P1-N1	105.7 (3)	C17-C18-C19	104.9 (9)
F1-P1-N3	107.0 (2)	C18-C19-C20	106.1 (9)
F1-P1-C1	103.2 (3)	O1-C20-C19	110.7 (8)
N1-P1-N3	118.0 (3)	O2-C21-C22	105.3 (7)
N1-P1-C1	110.6 (3)	C21-C22-C23	106.0 (9)
N3-P1-C1	111.2 (3)	C22-C23-C24	106.4 (8)
F2-P2-N1	105.7 (3)	O2-C24-C23	105.3 (8)
F2-P2-N2	109.5 (4)	O3-C25-C26	105.4 (8)
F2-P2-C6	102.1 (3)	C25-C26-C27	106.2 (9)
N1-P2-N2	116.5 (3)	C26-C27-C28	107.9 (9)
N1-P2-C6	110.6 (3)	O3-C28-C27	106.9 (8)
N2-P2-C6	111.4 (3)	P3-B-C11	106.7 (5)
N2-P3-N3	112.7 (3)	P3-B-C13	105.8 (6)
N2-P3-B	115.4 (4)	P3-B-C15	106.5 (6)
N3-P3-B	114.3 (3)	C11-B-C13	112.7 (7)
C17-O1-C20	106.9 (7)	C11-B-C15	114.6 (8)
C17-O1-Li	126.8 (5)	C13-B-C15	110.0 (6)
C20-O1-Li	125.0 (5)	O1-Li-O2	96.3 (7)
C21-O2-C24	106.0 (7)	O1-Li-O3	108.6 (6)
C21-O2-Li	125.0 (6)	O1-Li-N3	116.5 (6)
C24-O2-Li	128.4 (7)	O2-Li-O3	102.2 (5)
C25-O3-C28	108.6 (6)	O2-Li-N3	113.5 (6)
C25-O3-Li	126.2 (6)	O3-Li-N3	117.1 (7)
C28-O3-Li	124.7 (6)		

[a] Numbers in parentheses are estimated standard deviations in the least significant digits.

narity, with atom N1 displaced 0.63 Å from the plane defined by the other five ring atoms. The corresponding displacement in **12** is 0.62 Å. This type of distortion is attributed to the presence of the transannular ferrocenyl unit.

Table IV. Table of Positional Parameters and Their Estimated Standard Deviations

atom	*x*	*y*	*z*	*B*, Å^2
H	0.9707	0.0606	−0.0566	5[a]
H21	0.8187	0.0926	0.0996	5[a]
H31	0.8204	0.1030	0.3166	5[a]
H41	0.8282	0.1931	0.3606	5[a]
H51	0.8413	0.2375	0.1799	5[a]
H71	1.1424	0.0883	0.2382	5[a]
H81	1.1470	0.1023	0.4578	5[a]
H91	1.1482	0.1927	0.4898	5[a]
H101	1.1459	0.2351	0.2985	5[a]
H111	1.1229	0.0580	−0.3222	5[a]
H112	1.1789	0.0787	−0.1855	5[a]
H121	1.2182	−0.0021	−0.1790	5[a]
H122	1.1260	0.0084	−0.1153	5[a]
H123	1.0700	−0.0121	−0.2520	5[a]
H131	0.8677	0.0202	−0.2803	5[a]
H132	0.7790	0.0626	−0.3553	5[a]
H141	0.7652	0.0007	−0.4938	5[a]
H142	0.8257	0.0457	−0.5270	5[a]
H143	0.9144	0.0033	−0.4519	5[a]
H151	0.9441	0.1224	−0.4386	5[a]
H152	0.8606	0.1418	−0.3727	5[a]
H161	0.9913	0.1974	−0.3825	5[a]
H162	1.0276	0−.1843	−0.2421	5[a]
H163	1.1111	0.1649	−0.3080	5[a]
Fe	0.9873 (1)	0.15836 (4)	0.2581 (1)	2.55 (3)
P1	0.8610 (2)	0.17845 (6)	−0.0439 (2)	2.15 (4)
P2	1.1134 (2)	0.17355 (7)	0.0603 (2)	2.60 (5)
P3	0.9763 (2)	0.09995 (6)	−0.1096 (2)	2.14 (4)
F1	0.7491 (3)	0.2131 (1)	−0.1277 (4)	3.4 (1)
F2	1.2335 (3)	0.2039 (2)	0.0700 (4)	4.1 (1)
O1	0.6052 (4)	0.0433 (2)	−0.2342 (5)	3.9 (1)
O2	0.5303 (4)	0.1363 (2)	−0.1584 (4)	3.7 (1)
O3	0.5693 (4)	0.1374 (2)	−0.4052 (4)	3.6 (1)
N1	0.9906 (5)	0.2078 92)	−0.0068 (5)	2.2 (1)
N2	1.1104 (5)	0.1244 (2)	−0.0073 (5)	2.9 (1)
N3	0.8431 (5)	0.1298 (2)	−0.1223 (5)	2.1 (1)
C1	0.8300 (6)	0.1691 (2)	0.0905 (6)	2.1 (2)
C2	0.8226 (6)	0.1222 (3)	0.1397 (6)	2.9 (2)
C3	0.8231 (7)	0.1283 (3)	0.2622 (7)	4.1 (2)
C4	0.8297 (7)	0.1787 (3)	0.2881 (6)	3.8 (2)
C5	0.8353 (6)	0.2033 (3)	0.1849 (7)	3.4 (2)
C6	1.1483 (6)	0.1646 (3)	0.2246 (7)	2.9 92)
C7	1.1457 (7)	0.1189 (3)	0.2777 (7)	3.9 (2)
C8	1.1469 (8)	0.1267 (3)	0.4004 (7)	4.6 (2)
C9	1.1460 (8)	0.1775 (3)	0.4169 (7)	4.5 (2)
C10	1.1470 (7)	0.2017 (3)	0.3104 (7)	3.5 (2)
C11	1.1128 (7)	0.0576 (3)	−0.2431 (8)	5.5 (2)
C12	1.1361 (11)	0.0096 (4)	−0.1933 (12)	10.4 (4)
C13	0.8554 (8)	0.0451 (4)	−0.3405 (7)	6.6 (3)
C14	0.8420 (11)	0.0231 (5)	−0.4618 (11)	10.3 (4)
C15	0.9484 (11)	0.1304 (4)	−0.3557 (8)	9.9 (3)
C16	1.0169 (12)	0.1718 (3)	−0.3250 (9)	8.4 (3)
C17	0.4814 (8)	0.0226 (3)	−0.3007 (9)	5.3 (3)
C18	0.4754 (9)	−0.0184 (4)	−0.2207 (11)	7.8 (3)
C19	0.6126 (11)	−0.0322 (4)	−0.1439 (13)	10.9 (5)
C20	0.6863 (9)	0.0069 (3)	−0.1470 (11)	7.5 (3)
C21	0.4962 (7)	0.1101 (3)	−0.0698 (7)	4.6 (2)
C22	0.4562 (8)	0.1478 (4)	−0.0023 (8)	5.4 (3)
C23	0.4243 (10)	0.1907 (4)	−0.0829 (9)	8.3 (3)
C24	0.4467 (8)	0.1776 (3)	−0.1962 (9)	5.5 (3)
C25	0.5129 (8)	0.1091 (3)	−0.5197 (8)	5.2 (3)
C26	0.5339 (10)	0.1382 (4)	−0.6183 (9)	7.5 (3)
C27	0.5550 (11)	0.1863 (4)	−0.5736 (9)	8.2 (3)
C28	0.5735 (12)	0.1859 (3)	−0.4384 (9)	7.9 (3)
B	0.9756 (8)	0.0820 (3)	−0.2745 (7)	2.8 (2)
Li	0.6512 (11)	0.1121 (4)	−0.2304 (12)	3.3 (3)

[a] Anisotropically refined atoms are given in the form of the isotropic equivalent displacement parameter defined as $(4/3)[a^2B(1,1) + b^2B(2,2) + c^2B(3,3) + ab(\cos\gamma)B(1,2) + ac(\cos)\beta)B(1,3) + bc(\cos\alpha)B(2,3)]$.

Electronic Structures of Phosphazene Anions 6, 11, and 15. The reactivity of the fluorophosphazene anion **6** is consistent with the presence of a nucleophilic phosphorus(V) atom in the ring skeleton. By contrast, the

Table V. Bond Lengths and Angles for 12, 15, and $(NPF_2)_3$

compd	N–P, Å	P–F, Å	N–P–N, deg	P–N–P, deg	ref
12	1.592[a]	1.547	115.2	111.0	17c
	1.558	1.538	120.5	118.4	
15	1.572[a]	1.564	116.5	110.4	1
	1.674		112.7	118.7	
$(NPF_2)_3$	1.57	1.52	119.4	120.4	18

[a] Numbers in these rows represent values for lengths and angles obtained at the phosphorus atom bearing both fluorine and ferrocenyl substituents.

negative charges in the hydridophosphazene anions 11 and 15 appear to be localized on skeletal nitrogen atoms. Thus, although reaction of 6 with organic or organometallic electrophiles gave products from the replacement of a triethylborane group at phosphorus, species 11 and 15 yielded a complex mixture of products. Furthermore, the reaction of 15 with 2-propanol led to protonation at nitrogen to produce 17. Presumably, this is a consequence of the inability of the relatively electropositive hydrogen substituent to stabilize phosphorus in the +5 oxidation state. Thus, loss of the stabilizing electronegative fluorine substituent geminal to the triethylborane group results in preferential localization of the negative charge on skeletal nitrogen. In these cases, the skeletal phosphorus atom that bears the triethylborane group can be regarded as possessing a +3 oxidation state.

In order to provide further evidence for the existence of a P(III) site in 11, the magnitudes of J_{PH} coupling constants for different P(III) and P(V) hydrido species were measured and compared. The hydridophosphazene species $N_3P_3(OCH_2CF_3)_5H$ (9) has a relatively large P(V)–H coupling constant of approximately 540 Hz. By contrast, the corresponding value for the hydridophosphazene anion 11 is much smaller (only 320 Hz). The ^{31}P NMR spectrum of the P(III) hydride Ph_2PH was also obtained in order to provide additional evidence that the coupling constant differences can be attributed to a difference in the oxidation state of the phosphorus atoms. The ^{31}P NMR spectrum of Ph_2PH shows a doublet at 38.3 ppm with a one-bond PH coupling constant of 240 Hz. Moreover, when the phosphine is complexed to BEt_3, the doublet resonance broadens, due to unresolved coupling to boron. The coupling constant increases only slightly to 270 Hz. The magnitude of the J_{PH} coupling constant in 11 could be an indication of a phosphorus atom in the +3 oxidation state.[21]

Conclusions

The formation of phosphazene anions derived from fluorophosphazenes is remarkably facile and provides access to some novel small-molecule species. These compounds include fluorophosphazene anions that possess a synthetically useful nucleophilic P(V) center and hydridophosphazene anions that contain a P(III) center. In general, the P(III) species undergo ring cleavage reactions with electrophiles.

Attempts to increase the loading of the anionic sites on the phosphazene ring by the addition of excess $Li[BEt_3H]$ to solutions of 6 appear to yield hydridophosphazene monoanions (11), dianions, and trianions, and complex products that are associated with cleavage of the P–N ring. This suggests that, although the fluorophosphazene anions are substantially easier to form and provide significant synthetic advantages, these species also suffer from some of the same limitations as their chlorophosphazene counterparts.

(21) *Phosphorus-31 NMR Spectroscopy in Stereochemical Analysis*; Verkade, J. G., Quin, L. D., Eds.; Methods in Stereochemical Analysis; VCH Publishers: Deerfield Beach, FL, 1987; Vol. 8.

Table VI. Summary of Crystal Data and Collection Parameters for 15[a]

formula	$C_{28}H_{48}BF_2FeLiN_3O_3P_3$
MW	678.76
cryst size, mm	0.37 × 0.54 × 0.43
space group	$P2_1/c$
a, Å	11.363 (3)
b, Å	27.701 (9)
c, Å	11.667 (5)
β, deg	115.42 (4)
V, Å^3	3316.8
Z	4
D(cald), g/cm^3	1.015
radiation	Cu Kα
T, K	223
no. of data used [$I > 3\sigma(I)$]	2276
R, $R_w = (\sum^5 2_5/\sum wF_o^2)^{1/2}$	0.058, 0.078

[a] The structure was solved by direct methods and refined by full-matrix least squares calculations.

Experimental Section

Equipment and Materials. ^{31}P (36.2 MHz), ^{19}F (84.3 MHz), and ^{13}C (22.5 MHz) NMR spectra were obtained with use of a JEOL FX 90Q spectrometer; references were relative external 85% H_3PO_4, C_6H_5F, and $SiMe_4$, respectively. High-field ^{31}P NMR (145.8 MHz) and ^1H NMR (360.0 MHz) spectra were obtained by using a Bruker WP 360 spectrometer. Infrared spectra were recorded by use of a Perkin-Elmer 1710 FTIR interfaced with a Perkin-Elmer 3600 data station.

Hexachlorocyclotriphosphazene was provided by Ethyl Corp. and was recrystallized from hexane and sublimed (30 °C, 0.05 mmHg) before use. Hexafluorocyclotriphosphazene was prepared by previously reported methods and was dried by fractional distillation from CaH_2, b.p. 48–52 °C.[22] $N_3P_3F_4(\eta\text{-}C_5H_4)_2Fe$ was prepared according to the method of Allcock, Riding, and Lavin.[17c] THF (Omnisolv) was distilled from sodium benzophenone ketyl. 2,2,2-Trifluoroethanol (Halocarbon) was distilled from anhydrous BaO. Methyl iodide, benzyl bromide, and cyclopentadienyldicarbonyliron iodide (Aldrich) were dried by distillation onto sieves from BaO and heating under vacuum, respectively. $Li[BEt_3H]$ (1 M solution in THF) was obtained from Aldrich and was used as received. All manipulations were carried out by using standard Schlenk line techniques. Elemental analyses were obtained from Galbraith Laboratories, Knoxville, TN.

X-ray Crystal Data. Crystals of 15 were grown in the absence of light from a THF/diethyl ether solution for 14 days at 0 °C. X-ray crystallographic data were collected on an Enraf-Nonius CAD4 diffractometer controlled by a PDP 11/44 computer. Additional details of the X-ray analysis are available in Table VI and in the supplementary material.

Synthesis of $N_3P_3(OCH_2CF_3)_5Me$ (7). To a solution of $(NPF_2)_3$ (1.0 g, 4.0 mmol) in dry THF (~150 mL) was added 8.0 mL (8.0 mmol) of $Li[BEt_3H]$ over a 10-min period. Hydrogen gas was evolved during this step. A ^{31}P NMR spectrum of the solution was obtained after approximately 30 min. The spectrum confirmed the formation of the fluorophosphazene anion 6 (see Figure 1c). To the anion solution was added methyl iodide (12.0 mmol), and the reaction mixture was stirred at 25 °C for 8–10 h. A ^{31}P NMR spectrum of this reaction mixture showed that the anion had reacted completely. To this solution was added 30 mmol of $NaOCH_2CF_3$ prepared by the interaction of Na^0 with dry trifluoroethanol. The reaction mixture was heated at 66 °C for 6 h. ^{31}P NMR spectroscopy confirmed that all the fluorine atoms had been replaced by CF_3CH_2O groups. The product was isolated by removal of the THF, followed by extraction with CH_2Cl_2. Removal of the methylene chloride produced a light yellow oil, which was purified by column chromatography on silica gel with hexane/CH_2Cl_2 (4:1). Mass spectral data: m/z = 645, identified fragments included loss of F, CH_3, and OCH_2CF_3 groups.

(22) Schmutzler, R. *Inorg. Synth.* **1967**, *9*, 75.

Anal. Calcd (based on $C_{11}H_{13}F_{15}N_3O_5P_3$): C, 20.48; H, 2.04; N, 6.83. Found: C, 20.90; H, 1.93; N, 7.01. Other characterization data are listed in Table I.

Synthesis of $N_3P_3(OCH_2CF_3)_5CH_2Ph$ (8). This compound was prepared from 6 and $PhCH_2Br$ by a procedure similar to that used for 7. Purification was achieved by column chromatography using hexane/CH_2Cl_2 (5:1). Mass spectral data: m/z = 721, identified fragments included loss of F, CH_2PH, and OCH_2CF_3 groups. Anal. Calcd (based on $C_{17}H_{17}F_{15}N_3O_5P_3$): C, 28.31; H, 2.38; N, 5.83. Found: C, 29.04; H, 2.40; N, 5.90. Other characterization data are listed in Table I.

Synthesis of $N_3P_3(OCH_2CF_3)_5H$ (9). This compound was prepared in a manner similar to that described previously. After the formation of the anion 6 was confirmed by ^{31}P NMR spectroscopy, dry trifluoroethanol (12 mmol) was added to the reaction mixture. Following 6–8 h of reaction, a ^{31}P NMR spectrum showed that the anion had reacted completely. To this solution was added excess $NaOCH_2CF_3$, and the solution was refluxed for 6 h. The product was isolated and purified by column chromatography using hexane/methylene chloride as the eluting solvent. Mass spectral data: m/z = 631, identified fragments included loss of F, H, and OCH_2CF_3 groups. Anal. Calcd (based on $C_{10}H_{11}F_{15}N_3O_5P_3$): C, 19.03; H, 1.76; N, 6.67. Found: C, 18.83; H, 2.19; N, 6.85. Other characterization data are listed in Table I.

Synthesis of $N_3P_3(OCH_2CF_3)_5[CpFe(CO)_2]$ (10). This compound was prepared from 6 and $CpFe(CO)_2I$ by a procedure similar to that used for 7. The compound was isolated by column chromatography using hexane/methylene chloride as the eluting solvent. Species 10 was recrystallized from ethanol/Et_2O (5:1). Mass spectral data: m/z = 807, identified fragments included loss of F, $CpFe(CO)_2$, CO, and OCH_2CF_3 groups. Anal. Calcd (based on $C_{17}H_{15}F_{15}FeN_3O_7P_3$): C, 25.30; H, 1.88; N, 5.21. Found: C, 25.50; H, 2.12; N, 4.90. Other characterization data are listed in Table I.

Reaction of $N_3P_3F_4(\eta\text{-}C_5H_4)_2Fe$ with $Li[BEt_3H]$. To a cooled (5 °C) solution of $N_3P_3F_4(\eta\text{-}C_5H_4)_2Fe$ (1.40 g, 3.54 mmol) in THF (20 mL) was added a 1.0 M solution of $Li[BEt_3H]$ in the same solvent (11.0 mL, 11.0 mmol). Hydrogen evolved, and the solution was allowed to warm to room temperature and was stirred overnight. Analysis of the reaction mixture by ^{31}P NMR spectroscopy revealed the presence of species 15 (ca. 75%) together with small quantities of compounds 17 and 18. Concentration of the reaction solution to ca. 5 mL and dilution with diethyl ether (30 mL) followed by cooling to −20 °C for 14 days in the absence of light afforded yellow-orange crystals, which become opaque on exposure to light or on warming to room temperature.

Protonation of $[N_3P_3F_2H(BEt_3)(\eta\text{-}C_5H_4)_2Fe]^-$ (15) with ^iPrOH. To a solution of 15 (5 mmol), generated as above in THF (20 mL), was added excess ^iPrOH (2 mL). Analysis of the reaction mixture by ^{31}P NMR spectroscopy showed that 15 had been converted to 17. Solutions of 17 decomposed at room temperature during 24 h to yield metallic iron and a complex uncharacterized mixture.

Acknowledgment. The support of the U.S. Army Research Office and the Air Force Office of Scientific Research is greatly appreciated. We also acknowledge the suggestions of M. N. Mang.

Supplementary Material Available: Table S-I, giving general displacement parameter expressions for 15 (2 pages); Table S-II, listing structure factors (23 pages). Ordering information is given on any current masthead page.

Synthesis of Strained Ferrocenylorganocyclophosphazenes: X-ray Crystal Structures of $N_3P_3(OCH_2CF_3)_4(\eta\text{-}C_5H_4)_2Fe$, $N_3P_3(OPh)_4(\eta\text{-}C_5H_4)_2Fe$, and $N_3P_3Ph_2(OCH_2CF_3)_2(\eta\text{-}C_5H_4)_2Fe$

Harry R. Allcock,* Jeffrey A. Dodge, Ian Manners, Masood Parvez, Geoffrey H. Riding, and Karyn B. Visscher

Department of Chemistry, The Pennsylvania State University, University Park, Pennsylvania 16802

Received November 16, 1990

A series of transannular ferrocenylcyclotriphosphazenes were synthesized for studies of the relationship between molecular structure and polymerization behavior. Species $N_3P_3(OCH_2CF_3)_4(\eta\text{-}C_5H_4)_2Fe$ and $N_3P_3(OPh)_4(\eta\text{-}C_5H_4)_2Fe$ were synthesized by the reaction of $N_3P_3F_4(\eta\text{-}C_5H_4)_2Fe$ with $NaOCH_2CF_3$ and NaOPh, respectively. Cyclic trimers $N_3P_3R(OCH_2CF_3)_3(\eta\text{-}C_5H_4)_2Fe$ [R = OPh, R = Me, R = Ph (*gem* to Cp) and R = Ph (non-*gem* to Cp)] were prepared by reactions of the appropriate fluoroferrocenylphosphazene precursors $[N_3P_3(OPh)F_3(\eta\text{-}C_5H_4)_2Fe$, $N_3P_3MeF_3(\eta\text{-}C_5H_4)_2Fe$, $N_3P_3PhF_3(\eta\text{-}C_5H_4)_2Fe$, and $N_3P_3PhF_3(\eta\text{-}C_5H_4)_2Fe]$ with $NaOCH_2CF_3$. The synthesis of $N_3P_3Ph_2(OCH_2CF_3)_2(\eta\text{-}C_5H_4)_2Fe$, (Ph groups non-*gem* to Cp) was achieved via the reaction of *gem*-$N_3P_3F_4Ph_2$ with dilithioferrocene to give $N_3P_3Ph_2F_2(\eta\text{-}C_5H_4)_2Fe$, followed by treatment with $NaOCH_2CF_3$. Treatment of $N_3P_3Ph_2F_2(\eta\text{-}C_5H_4)_2Fe$ with $NaOCH_2CF_3$ yielded $N_3P_3Ph_2(OCH_2CF_3)_2(\eta\text{-}C_5H_4)_2Fe$ (Ph groups *gem* to Cp). A 1-equiv amount of NaOPh reacts with $N_3P_3F_4(\eta\text{-}C_5H_4)_2Fe$ to form a mixture of *cis*- and *trans*-$N_3P_3(OPh)F_3(\eta\text{-}C_5H_4)_2Fe$. The molecular structures of $N_3P_3(OCH_2CF_3)_4(\eta\text{-}C_5H_4)_2Fe$, $N_3P_3(OPh)_4(\eta\text{-}C_5H_4)_2Fe$, and $N_3P_3Ph_2(OCH_2CF_3)_2(\eta\text{-}C_5H_4)_2Fe$ were determined by single-crystal X-ray diffraction. All were found to possess nonplanar, strained cyclotriphosphazene rings. Crystals of $N_3P_3(OCH_2CF_3)_4(\eta\text{-}C_5H_4)_2Fe$ are monoclinic with space group $P2_1/c$, with a = 9.529 (5) Å, b = 14.515 (2) Å, c = 19.012 Å, β = 97.94 (2)°, V = 2605.8 Å^3, and Z = 4. Crystals of $N_3P_3(OPh)_4(\eta\text{-}C_5H_4)_2Fe$ are orthorhombic of space group $P2_12_12_1$ with a = 9.890 (2) Å, b = 15.962 (3) Å, c = 19.629(3) Å, V = 3098.8 Å^3, and Z = 4. The diphenyl species, $N_3P_3Ph_2(OCH_2CF_3)_2(\eta\text{-}C_5H_4)_2Fe$, crystallizes in the trigonal space group $R3$ (hexagonal axes) with a = 23.954 (8)Å, b = 23.94 (1) Å, c = 13.17 (1) Å, V = 6544 Å^3, and Z = 9.

One of the main routes for the synthesis of stable high-polymeric phosphazenes is via the ring-opening polymerization of cyclic chloro- or fluorophosphazenes such as $[NPCl_2]_3$ or $[NPF_2]_3$, followed by replacement of the halogen atoms in the polymer by organic side groups.[1-3] However, until recently, all attempts to prepare poly(organophosphazenes) by the polymerization of cyclic phos-

(1) Allcock, H. R. *Phosphorus-Nitrogen Compounds*; Academic Press: New York, 1972.

0276-7333/91/2310-3098$02.50/0